Performances of a large mass ZnSe bolometer to search for rare events

2013 JINST 8 P05021

(http://iopscience.iop.org/1748-0221/8/05/P05021)

PUBLISHED BY IOP PUBLISHING FOR SISSA MEDIALAB

RECEIVED: *March 21, 2013*
ACCEPTED: *May 13, 2013*
PUBLISHED: *May 28, 2013*

Performances of a large mass ZnSe bolometer to search for rare events

J.W. Beeman,[a] **F. Bellini,**[b,c] **L. Cardani,**[b,c,1] **N. Casali,**[d,e] **I. Dafinei,**[c] **S. Di Domizio,**[h] **F. Ferroni,**[b,c] **L. Gironi,**[f,g] **A. Giuliani,**[i] **S. Nagorny,**[e] **F. Orio,**[c] **L. Pattavina,**[e] **G. Pessina,**[g] **G. Piperno,**[b,c] **S. Pirro,**[g] **E. Previtali,**[g] **C. Rusconi,**[g] **C. Tomei**[c] **and M. Vignati**[c]

[a] *Lawrence Berkeley National Laboratory, Berkeley, California 94720, U.S.A.*
[b] *Dipartimento di Fisica, Università di Roma La Sapienza, I-00185 Roma, Italy*
[c] *INFN - Sezione di Roma, I-00185 Roma, Italy*
[d] *Dipartimento di Scienze Fisiche e Chimiche, Università degli studi dell'Aquila, I-67100 Coppito (AQ), Italy*
[e] *INFN - Laboratori Nazionali del Gran Sasso, I-67010 Assergi (AQ), Italy*
[f] *Dipartimento di Fisica, Università di Milano Bicocca, I-20126 Milano, Italy*
[g] *INFN - Sezione di Milano Bicocca, I-20126 Milano, Italy*
[h] *INFN - Sezione di Genova, I-16146 Genova, Italy*
[i] *CSNSM, Centre de Spectrométrie Nucléaire et de Spectrométrie de Masse, Bâtiment 108, Campus d'Orsay, 91405 Orsay, France*

E-mail: laura.cardani@roma1.infn.it

[1] Corresponding author.

doi:10.1088/1748-0221/8/05/P05021

2013 JINST 8 P05021

ABSTRACT: Scintillating bolometers of ZnSe are the baseline choice of the LUCIFER experiment, whose aim is to observe the neutrinoless double beta decay of ^{82}Se. The independent read-out of the heat and scintillation signals allows to identify and reject α particle interactions, the dominant background source for bolometric detectors. In this paper we report the performances of a ZnSe crystal operated within the LUCIFER R&D. We measured the scintillation yield, the energy resolution and the background in the energy region where the signal from 0νDBD decay of ^{82}Se is expected with an exposure of $9.4\,\mathrm{kg}\cdot\mathrm{days}$. With a newly developed analysis algorithm we improved the rejection of α events, and we estimated the increase in energy resolution obtained by the combination of the heat and light signals. For the first time we measured the light emitted by nuclear recoils, and found it to be compatible with zero. We conclude that the discrimination of nuclear recoils from β/γ interactions in the WIMPs energy region is possible, but low-noise light detectors are needed.

KEYWORDS: Double-beta decay detectors; Dark Matter detectors (WIMPs, axions, etc.); Particle identification methods; Calorimeters

ARXIV EPRINT: 1303.4080

2013 JINST 8 P05021

Contents

2013 JINST 8 P05021

1 Introduction

Bolometers are solid state detectors in which the energy release coming from particle interactions is converted to heat and measured via their rise in temperature. They can provide excellent energy resolution and low background, and are used in particle physics experiments searching for rare processes, such as neutrinoless double beta decay (0νDBD) and Dark Matter interactions.

In the last years, an extensive R&D allowed to increase the mass of bolometric detectors and, at the same time, to understand and reduce the sources of background. The largest bolometric detector operated up to now, Cuoricino, was made of about 40.7 kg of TeO_2 and took data from 2003 to 2008, demonstrating the potential of this technique [1, 2]. The evolution of Cuoricino, CUORE, will search for the 0νDBD of ^{130}Te [3, 4] using an array of 988 TeO_2 bolometers of 750 g each. Operated at a temperature of about 10 mK, these detectors provide an energy resolution of a few keV over their energy range, extending from a few keV up to several MeV. The measured resolution at the Q-value of the decay ($Q = 2527$ keV [5]) is about 5 keV FWHM; together with the low background and the large mass of the experiment, this will provide a 1σ sensitivity to the 0νDBD of ^{130}Te of the order of 10^{26} years.

To further increase the sensitivity, an intense R&D is being pursued to lower the background in the 0νDBD region. The main source of background is due to α particles, coming from radioactive contaminations of the materials facing the bolometers [6]. A way to discriminate this background is to use a scintillating bolometer [7]. In such a device the simultaneous and independent read-out of the heat and the scintillation light permits to discriminate events due to β/γ, neutron and α interactions thanks to their different scintillation properties. Unfortunately TeO_2 crystals do not scintillate and different compounds are being studied. Among these are $CdWO_4$ [8] (0νDBD candidate ^{116}Cd, $Q = 2814$ keV [5]), ZnSe [9] (^{82}Se, $Q = 2997$ keV [10]), and $ZnMoO_4$ [11–14] (^{100}Mo, $Q = 3034$ keV [15]).

In this paper we investigate the performances of a ZnSe scintillating crystal for the 0νDBD search in terms of energy resolution, capability of discriminating α particles and internal radioactive contaminations. We also study the light emitted by nuclear recoils and β/γ interactions at 100 keV, discussing the possibility of using ZnSe bolometers as Dark Matter detectors.

2 Experimental setup

The data here presented come from a series of runs performed at Laboratori Nazionali del Gran Sasso (LNGS) in Italy, inside the CUORE R&D facility. The bolometer under study is a 431 g ZnSe crystal with cylindrical shape (height 44.3 mm and diameter 48.5 mm). The synthesis of the ZnSe powder, including purification and formatting for crystal growth [16, 17], was made in ultra-clean fused quartz reactors at SmiLab Svitlovodsk (Ukraine).

To detect the scintillation light, many different light detectors (LD) were faced to the ZnSe crystal. They consist of pure Germanium slabs of 50 mm diameter and with variable thickness (300–600 μm) and they were operated as bolometers to obtain good performances at cryogenic temperatures [18]. We covered a face of the LD with a thin layer of SiO_2 (60 nm) and obtained an increase of the light absorption by $\sim$ 16–20%, as already observed in ref. [19]. Moreover, we measured an increase of $\sim$ 25% in the collection efficiency by surrounding the crystal with a 3M VM2002 reflecting foil.

The temperature sensors of both the ZnSe and LD were Neutron Transmutation Doped (NTD) Germanium thermistors [20], coupled to the ZnSe and Ge surfaces by means of epoxy glue spots. For redundancy, the ZnSe crystal was equipped with two sensors, in the following referred as ZnSe-L and ZnSe-R. The detectors were held in a copper structure by Teflon (PTFE) supports and thermally coupled to the mixing chamber of a dilution refrigerator which kept the system at a temperature around 10 mK. To read the signals, the thermistors were biased with a constant current. The voltage signals, amplified and filtered by means of an anti-aliasing 6-pole active Bessel filter (120 dB/decade), were fed into a NI PXI-6284 18-bits ADC operating at a sampling frequency of 2 kHz. The Bessel cutoff was set at 120 Hz for the LDs, and at 70 Hz for the ZnSe. Further details on the cryogenic facility and the electronic read-out can be found in refs. [21–23].

The trigger was software generated on each bolometer. When it fired, waveforms 5 s long on the ZnSe and 250 ms long on the LD were digitized and saved on disk. In addition, for every trigger occurring on the ZnSe, the LD waveform was acquired irrespective of its trigger. The off-line analysis computes the pulse height as well as pulse shape parameters based on the optimum filter algorithm [24, 25]. In addition, the amplitude of the light signals is computed with an algorithm that allows to lower the energy threshold of the LD using the knowledge of the signal time delay with respect to the ZnSe (see details in ref. [26]).

Compared to TeO_2 crystals, we observed that the ZnSe bolometer cooled very slowly, likely because of a heat capacitance excess at low temperature. Indeed, despite of the fact that the cryostat temperature was kept constant, the temperature drift of the ZnSe was large enough to influence the detector response still after 30 days of data-taking (figure 1). The resistance of the thermistor, which has a steep dependence on the temperature, increased of about 6% during this data acquisition period, resulting in a corresponding increase in the signal height. This behavior was also observed in bolometers made of BGO crystals [27].

2013 JINST 8 P05021

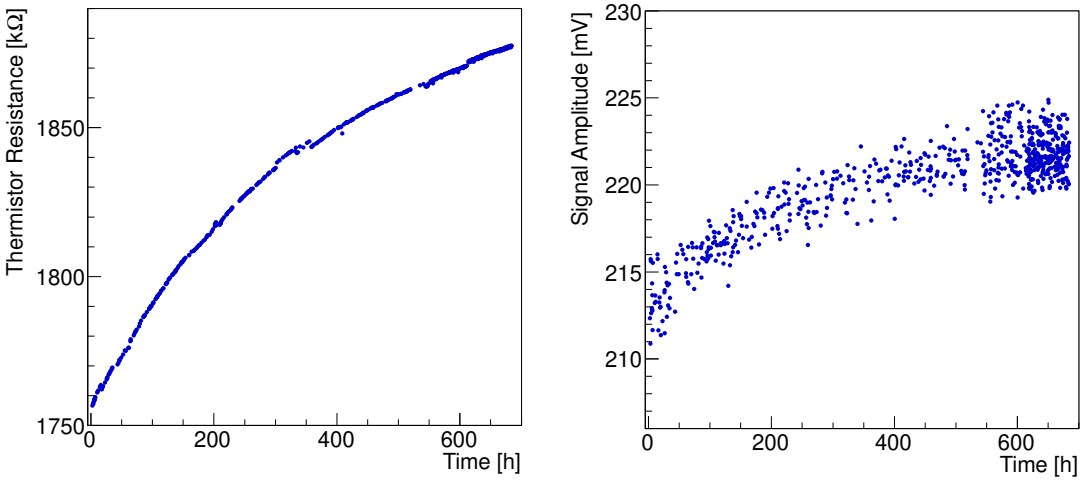

Figure 1. Change in the thermistor response induced by the slow cooling of the ZnSe bolometer, whose temperature decreased of about 1% during the first 700 hours of measurement. Left: increase of the thermistor resistance due to the cooling of the crystal. Right: amplitude of pulses with energy of about 1460 keV as a function of time. In the last 150 hours a calibration measurement was performed, resulting in a higher rate.

The calibration of the ZnSe pulse amplitude was performed by means of a ^{228}Th γ-source placed inside the cryostat external lead shield. We observed that the calibration function derived from γ peaks was not applicable to energy deposits induced by α particles, which were shifted by $+22\%$ with respect to their nominal energy. For this reason, in the following we will refer to the energy estimated from the γ calibration as "Energy$_{ee}$" (γs and electrons interact in the same way in the bolometer). When the calibration is derived from α peaks produced by the internal contaminations, the energy units will be indicated as "Energy$_{\alpha}$".

To evaluate the discrimination power between β/γ and α events in the energy region of interest (around 2997 keV [10]), an α-source was permanently placed close to the ZnSe crystal. The source consisted in an Uranium solution, covered with a thin mylar foil to absorb part of the αs energy and to produce a continuum spectrum in the range 1–4 MeV. Finally, during a calibration run, an AmBe neutron source was placed close to the detector in order to produce high energy γs.

The LD is calibrated with a ^{55}Fe source permanently faced to the LD surface opposite to the ZnSe. The source emits two X-rays at 5.9 and 6.5 keV.

The main features of the detectors are summarized in table 1. The rise and decay times of the pulses are defined as the time difference between the 90% and the 10% of the leading edge, and the time difference between the 30% and 90% of the trailing edge, respectively. The intrinsic energy resolution of the detector (σ_{baseline}) is estimated from the fluctuations of the detector baseline after the optimum filter application. Because of the better energy resolution, in the following we restrict our analysis to ZnSe-R.

2013 JINST 8 P05021

Table 1. Parameters of the bolometers. Amplitude of the signal before amplification (A_S), intrinsic energy resolution after the application of the optimum filter (σ_{baseline}), rise (τ_r) and decay (τ_d) times of the pulses. ZnSe-R is the thermistor chosen for the data analysis.

	A_S [μV/MeV]	σ_{baseline} [keV RMS]	τ_r [ms]	τ_d [ms]
ZnSe-L	10	5.2	5.6 ± 0.3	30 ± 4
ZnSe-R	50	2.4	5.7 ± 0.2	23 ± 2
LD	980	0.069	2.8 ± 0.1	9.4 ± 0.5

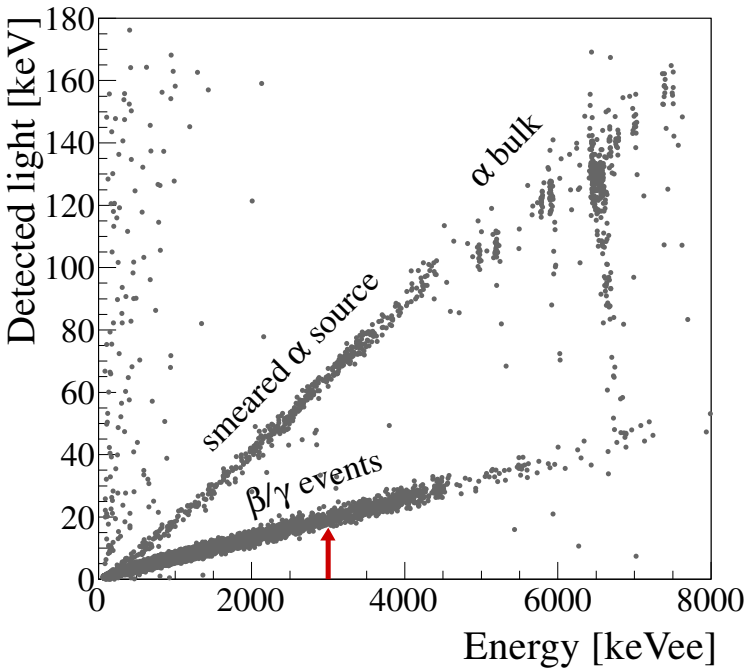

Figure 2. Detected Light vs Energy measured by the ZnSe in a calibration run. The energy axis has been calibrated using the most intense γ peaks. The ZnSe crystal is faced to a smeared α source (upper band) and to an AmBe neutron source (high energy γs in the lower band). The events characterized by low energy (below $\sim$ 1 MeV) and large detected light are particles that interacted in both the ZnSe and LD. The arrow points to the ^{82}Se Q-value (2997 keV).

3 Scintillation

The measured light as a function of the energy deposited in the ZnSe bolometer is shown in figure 2. Two regions can be clearly distinguished: the upper band, populated by α events provided by the smeared α source (continuum below $\sim 4.5\,\text{MeV}_{ee}$) and by internal and surface α contaminations, and the lower band, populated by γs produced by the neutron source. The Light Yield of β/γ events ($\text{LY}_{\beta/\gamma}$), defined as the amount of detected light per particle energy, does not depend on the energy. Fitting the β/γ band with a first order polynomial function, we obtain $\text{LY}_{\beta/\gamma} = 6.416 \pm 0.008$ keV/MeV. The Light Yield of αs (LY_α) is larger than $\text{LY}_{\beta/\gamma}$, unlike in other known scin-

2013 JINST 8 P05021

tillating crystals [28]. This behavior, already observed in other ZnSe crystals operated at cryogenic temperatures, is not yet fully understood. Nevertheless, as it will be shown in section 5, this does not limit the discrimination capability.

The continuum produced by the smeared α source was fitted with a first order polynomial function, resulting in $LY_{\alpha}^{smeared}$ = (29.70 $\pm$ 0.17) keV/MeV. The fit revealed the presence of an energy threshold for the scintillation, which is $E_{thresh}^{smeared}$ = (230 $\pm$ 12) keV_{α}. At larger energies, where only α peaks due to bulk contaminations are present, we obtained LY_{α}^{bulk} = (26.62 $\pm$ 0.86) keV/MeV and E_{thresh}^{bulk} = (180 $\pm$ 140) keV_{α}. The large error on the threshold is due to the large distance of the peaks from the origin, and does not allow a trustworthy comparison with the smeared source. However it is clear that LY_{α}^{bulk} is lower than $LY_{\alpha}^{smeared}$.

Understanding this discrepancy is not trivial. Indeed, for a given light detector and experimental set-up, the light yield includes not only the scintillation process that produces light, but also the light transport from the luminescent centre to the detector. Even if we are not able to disentangle these two processes, we performed some tests to investigate the effects on the discrepancy between LY_{α}^{bulk} and $LY_{\alpha}^{smeared}$ induced by the crystal self-absorption, by the reflection on the mylar foil and by the energy dependence. In detail:

- we checked whether the lower LY of bulk events could be due to the ZnSe self-absorption. This test was performed by placing the smeared source and the LD on opposite sides of the ZnSe, in such a way that the light emitted by αs impinging on the surface had to travel across the entire crystal before reaching the LD. The results of this test are the ones already reported above and show that $LY_{\alpha}^{smeared} > LY_{\alpha}^{bulk}$ even if we expect the maximum re-absorption of the scintillation light emitted by the smeared αs.

- we investigated a possible energy dependence of the LY by facing a ^{224}Ra source emitting high energy αs to the lateral surface of the ZnSe crystal, so that we could reproduce the same α particles from the bulk contamination and compare external and internal sources at the same energy. We obtained $LY_{\alpha}^{external}$ = (29.6 $\pm$ 0.1) keV/MeV from 4 to 6 MeV. This value is compatible with $LY_{\alpha}^{smeared}$ pointing to the hypothesis that the larger LY is not due to energy-dependent effects. We underline that this test was performed without reflecting foil, to make sure that the larger LY of external αs could not be attributed to the reflection on the mylar sheet.

The experimental data show that in every test the light yield from bulk interactions is lower than the one produced by external events. Further measurements are needed to deepen the understanding of this behavior, that could be attributed to an effectively higher light production (the bulk of a real crystal is different in many aspects from the thin layer close to the surface), or to the different light collection for surface/bulk events. Indeed, it is well known that the light collection is particularly non uniform when dealing with cylindrical crystals [29].

To evaluate the discrimination capability at the 0νDBD energy, we performed Gaussian fits to the light emitted in α and β/γ interactions, excluding the outliers due to α interactions in which a leakage of light is detected. From the fits we derived the mean value (μ) and the standard deviation (σ) of the light for both the α and β/γ interactions. Since the discrimination capability increases

2013 JINST 8 P05021

with energy (as one can see in figure 2), we calculated μ and σ in several energy intervals and fitted the energy dependence of μ(E) and σ(E) with polynomial functions.

We defined the Discrimination Potential as a function of the energy as:

$$DP(E) = \frac{\left|\mu_\alpha(E) - \mu_{\beta\gamma}(E)\right|}{\sqrt{\sigma^2_\alpha(E) + \sigma^2_{\beta\gamma}(E)}} \tag{3.1}$$

and found $DP = 17$ at 2997 keV. It has to be remarked that this is just and indication of the capability of rejecting the α background. As it can be noticed from figure 2, there is a considerable number of αs in which a large amount of light is lost. This behavior, likely due to surface effects, is particularly evident looking at the peak of ^{210}Po ($\sim 6.5\,\mathrm{MeV}_{ee}$), a common contaminant found on the ZnSe surface. The loss of light from α particles constitutes a non-negligible and hard to estimate background to β/γ events. As it will be shown in section 5, the pulse shape of the light signal carries information on the particle type, irrespective of the amount of light collected, allowing a safe identification of all α events.

We finally studied the LY at very low energies, which is of particular interest for experiments aiming at the detection of Dark Matter interactions. These experiments need to disentangle the signal produced by nuclear recoils below 30 keV (following the hypothesis that Dark Matter is made of WIMPs [30, 31]) from the background induced by β/γs. We analyzed the recoils following the α decay of ^{210}Po. Since this isotope is deposited on the surface, the α particle can escape without releasing energy, while the nuclear recoil is absorbed in the crystal. We observe events centered at $139.6 \pm 0.6\,\mathrm{keV_{ee}}$ in the ZnSe, i.e. 35% more energy than the nominal value (103 keV). The accuracy of the calibration function has been checked down to 511 keV, where it shows a deviation less than 1%. The extrapolation at lower energies is expected to maintain or reduce this deviation. From the fit in figure 3, we evaluate the light emitted by nuclear recoils as < 14 eV at 90% C.L., corresponding to $\mathrm{LY}_{nr} < 0.140\,\mathrm{keV/MeV}$ at 90% C.L. We evaluate the light emitted in the range $10 - 30\,\mathrm{keV_{nr}}$ as $< 1 - 4$ eV at 90% C.L. for nuclear recoils, and $90 - 260$ eV for β/γs.

In this test the energy threshold was not optimized and set at $70\,\mathrm{keV_{ee}}$ ($\sim 50\,\mathrm{keV_{nr}}$, assuming the 35% miscalibration), while to be competitive with present experiments it should be below $10\,\mathrm{keV_{nr}}$. Given the baseline fluctuation ($2.4\,\mathrm{keV_{ee}} = 1.7\,\mathrm{keV_{nr}}$) the required threshold could be reached with a trigger based on the optimum filter [32]. However, to obtain a DP between β/γs and nuclear recoils at least larger than 3, light detectors with baseline noise less than 20 eV RMS are needed. The light detectors currently being used are far from this value (see table 1) and obtaining resolutions better than 70 eV RMS does not seem to be achievable with the present technology. To search for Dark Matter interactions in ZnSe bolometers, new light detection technologies must be introduced.

4 Energy resolution

The energy resolution on the 0νDBD signal is estimated from γ lines, which produce the same bolometric and scintillation response of β particles. The energy resolution is found to be 13.4 ± 1.0 keV FWHM at 1461 keV (^{40}K contamination in the cryostat) and 16.3 ± 1.5 keV FWHM at 2615 keV (^{208}Tl from calibration). These values are worse than the baseline resolution, which is

2013 JINST 8 P05021

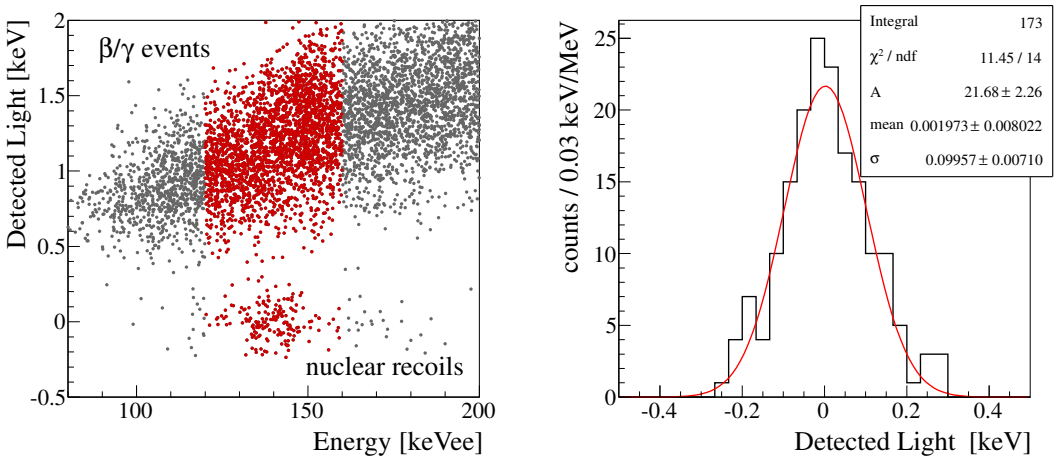

Figure 3. Left: energy region around the nuclear recoils from the ^{210}Po decay. The detected energy of the recoils, using the β/γ calibration function, is 35% larger than the nominal value (103 keV, see discussion in the text). Right: distribution of the light emitted from the nuclear recoils, selecting the events marked in red in the left figure and applying the cut Detected Light < 0.3 keV to remove the β/γ background.

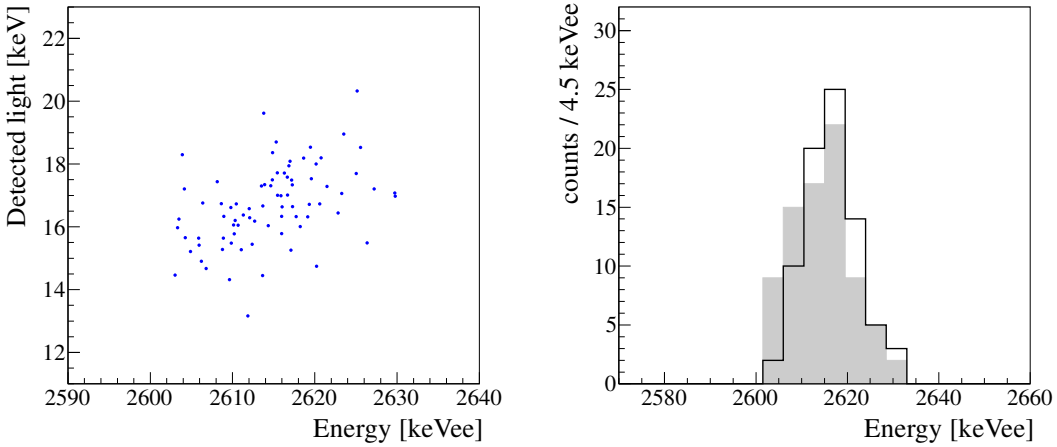

Figure 4. Left: correlation between the detected light and the energy released in the ZnSe for 2615 keV γ events. Right: energy distribution in the ZnSe before (gray) and after (black line) the combination with the light signal for the same events.

5.6 keV FWHM (see table 1). Looking at the detected light, we observe that there is a positive correlation with the energy measured in the ZnSe (figure 4 left). This is in contrast with other scintillating crystals, where the correlation is negative as expected from the conservation of energy [8]. Presently we are unable to explain this behavior, however we can take advantage from the correlation to improve the energy resolution.

The light L and energy E in the ZnSe are two correlated estimates of the same observable, i.e. the particle energy. Defining $L' = L/LY_{\beta/\gamma}$, we write the combined energy variable as:

$$E^{\text{comb}} = (1-w)\,E + w\,L' \,. \tag{4.1}$$

2013 JINST 8 P05021

Table 2. Energy resolution before and after the combination with the detected light.

	ZnSe [keV FWHM]	ZnSe and Light [keV FWHM]
1461 keV	13.4 ± 1.0	12.2 ± 0.8
2615 keV	16.3 ± 1.5	13.4 ± 1.3

The weight w that minimizes the variance of E^{comb} is:

$$w = \frac{\sigma_E^2(1-\rho\sigma_{L'}/\sigma_E)}{\sigma_E^2+\sigma_{L'}^2-2\rho\sigma_E\sigma_{L'}} \tag{4.2}$$

where σ_E^2 and $\sigma_{L'}^2$ are the variances of E and L', respectively, and ρ is the correlation between them. The expected variance of E^{comb} is then:

$$\sigma_{E^{\text{comb}}}^2 = \frac{\sigma_E^2\sigma_{L'}^2(1-\rho^2)}{\sigma_E^2+\sigma_{L'}^2-2\rho\sigma_E\sigma_{L'}}\,. \tag{4.3}$$

The application of this algorithm to data improves the energy resolution considerably, in particular at high energies where the energy resolution at 2615 keV improves from 16 to 13 keV FWHM (see table 2 and figure 4 right).

The resolutions of the light detector and of the ZnSe, as well as their correlation, depend on the energy. To apply eq. (4.1) to the entire energy spectrum, even where there are no peaks, a specific weight should be used (eq. (4.2)) at each energy. Since the resolutions and the correlation are slow functions of the energy, $w(E)$ has been estimated from polynomial functions fitting the energy dependence of σ_E, $\sigma_{L'}$ and ρ.

5 Pulse shape discrimination

Given the different light and heat yields of α and β/γ interactions, we tested whether also the shape of the signals carries information on the type of interacting particle [33, 34].

The average pulse of 2615 keV γ events in the ZnSe and the corresponding average scintillation pulse are shown in figure 5. The pulses are fitted with a model developed for TeO_2 bolometers [35, 36]. The model originally included the thermistor and electronics responses and the response of the bolometer, which describes the time development of the thermal phonon signal after an instantaneous energy absorption:

$$\Delta T(t) = A\left[-e^{-t/\tau_r}+\alpha e^{-t/\tau_{d1}}+(1-\alpha)e^{-t/\tau_{d2}}\right] \tag{5.1}$$

where A is the thermal amplitude, τ_r the rise time, $\tau_{d1,2}$ two decay constants and α is a weight ($0<\alpha<1$). In order to introduce the model in this work, the above equation has been modified to include energy releases that can not be considered instantaneous, such as the scintillation process.

A function which has been found to well reproduce the observed signals, both in the ZnSe and in the light detector, is:

$$\Delta T(t) = A_1\left[-e^{-t/\tau_r}+\alpha e^{-t/\tau_{d1}}+(1-\alpha)e^{-t/\tau_{d2}}\right]+A_2\left[-e^{-t/\tau_r}+e^{-t/\tau_{d3}}\right]. \tag{5.2}$$

2013 JINST 8 P05021

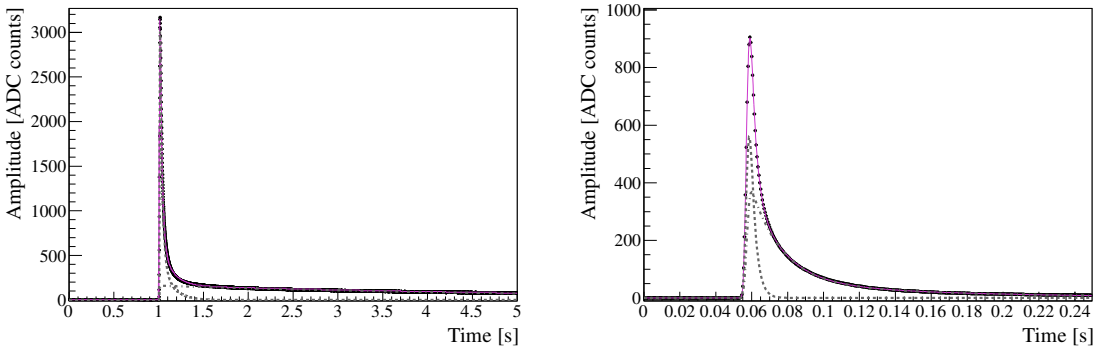

Figure 5. Average pulse of 2615 keV γ events in the ZnSe (left) and the corresponding average scintillation pulse (right). The dashed lines represent the fast and slow components of the fit function.

In figure 5 the total fit function and the two components are displayed. In the ZnSe the amplitude of the fast component is given by A_1, while the slow one by A_2. In the light detector the amplitude of the fast component is A_2, while the slow one is A_1. We suppose that the fast decay of the signal can be attributed to phonons, while the slow one is affected by the scintillation mechanism, which is different for α and β/γ interactions [37]. Applying the fit to each event, we noticed that the ratio of the slow and fast amplitude components (A_s/A_f) is related to the particle type. However the fit is too sensitive to the detector noise and to minimization problems and cannot be used to estimate a reliable discrimination parameter.

Following refs. [38, 39], we developed a bi-component optimum filter algorithm to lower the noise and improve the reliability of the parameter A_s/A_f. To explain the algorithm, we first remind to the reader the working principles of the standard optimum filter. Given a signal + noise waveform $f(t) = A \cdot S(t-t_0) + n(t)$, the best estimate of the amplitude A, under the hypothesis that the noise is stationary, is obtained from the χ^2 of the residuals in the frequency domain:

$$\chi^2 = \sum_{\omega} \frac{\left| f(\omega) - A \cdot S(\omega) e^{-i\omega t_0} \right|^2}{N(\omega)} \tag{5.3}$$

where $S(t)$ is the ideal pulse, estimated as the average pulse, and $N(\omega)$ is the noise power spectrum of the detector. The parameter t_0 accounts for any possible jitter between the observed signal and $S(t)$. Minimizing eq. (5.3) with respect to A, we obtain:

$$\hat{A}(t_0) = h \sum_{\omega} \frac{S^*(\omega) e^{i\omega t_0}}{N(\omega)} f(\omega) \tag{5.4}$$

where $h = [\sum_\omega |S(\omega)|^2/N(\omega)]^{-1}$. To estimate A, eq. (5.3) has to be minimized also with respect to t_0. This however cannot be done in an analytical form. It can be demonstrated that the minimum of eq. (5.3) with respect to t_0 and A is equivalent to the maximum of $\hat{A}(t_0)$. Since eq. (5.4) is an inverse Fourier transform on t_0, $\hat{A}(t_0)$ can be seen as the filtered signal in the time domain. In this domain, the best estimate of A ($\hat{A}$) can be extracted with a maximum search algorithm.

In the bi-component filter the waveform is decomposed as $f(t) = A_s S_s(t-t_0) + A_f S_f(t-t_0) + n(t)$, where in our case $S_s(t)$ and $S_f(t)$ are the ideal slow and fast components of the signal. The

2013 JINST 8 P05021

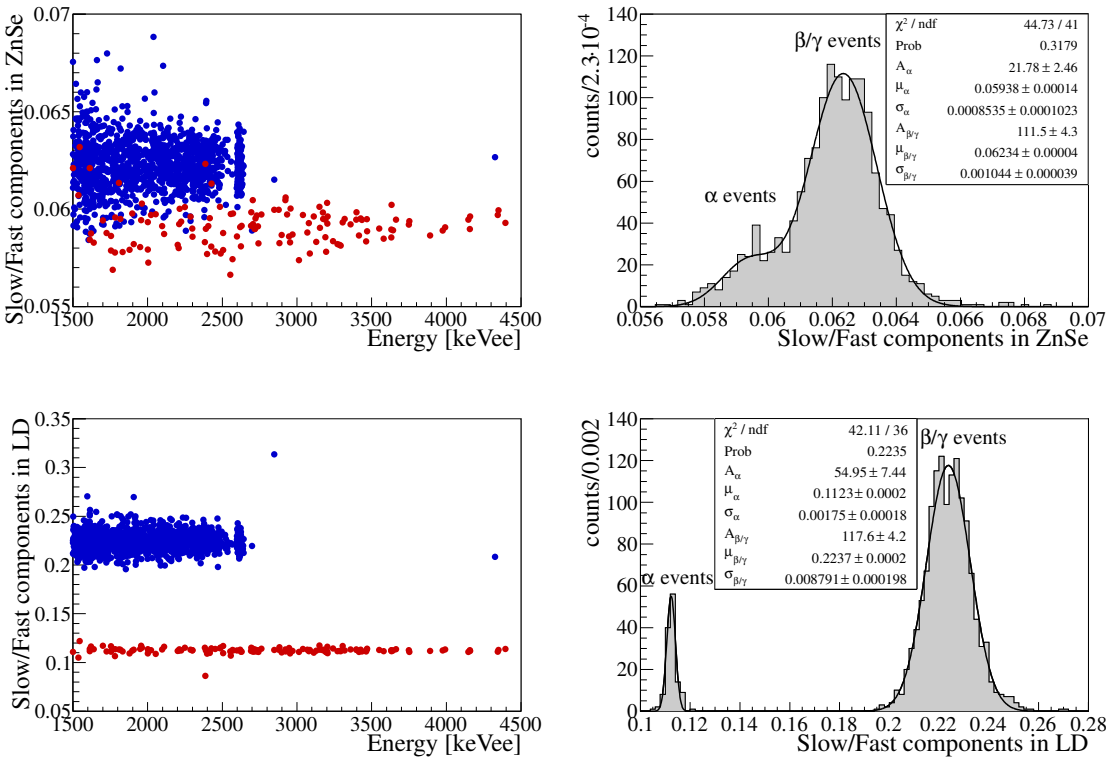

Figure 6. Left: ratio of the amplitudes estimated by the bi-component optimum filter algorithm as a function of the energy released in the ZnSe. The events tagged as α are marked with red, while β/γs with blue. Right: histogram of the ratio. Heat in ZnSe in the top row, light in the LD in the bottom row. The α and β/γ populations are well identified in the light detector but less in the ZnSe.

minimization of the χ^2 with respect to A_s and A_f gives:

$$\begin{pmatrix} \hat{A}_s(t_0) \\ \hat{A}_f(t_0) \end{pmatrix} = \begin{pmatrix} \sum |S_s|^2 N^{-1} & \sum (S_s^* S_f) N^{-1} \\ \sum (S_s^* S_f) N^{-1} & \sum |S_f|^2 N^{-1} \end{pmatrix}^{-1} \cdot \begin{pmatrix} \sum S_s^* e^{i\omega t_0} N^{-1} f \\ \sum S_f^* e^{i\omega t_0} N^{-1} f \end{pmatrix} \tag{5.5}$$

where the sums run over ω and S_s, S_f, N and f are to be intended in the frequency domain. In this case the minimum of the χ^2 with respect to t_0 does not correspond to the maxima of $\hat{A}_s(t_0)$ and $\hat{A}_f(t_0)$. Therefore we estimate $\hat{t}_0$ by scanning the χ^2 around $t_0 = 0$ and then evaluate $\hat{A}_f = \hat{A}_f(\hat{t}_0)$ and $\hat{A}_s = \hat{A}_s(\hat{t}_0)$.

The application of the bi-component optimum filter is shown in figure 6, using the fit components in figure 5 as estimates of $S_{s,f}(t)$. As the figure shows, the separation is very evident in the light detector and less evident in the ZnSe. In the case of the ZnSe we estimate $DP = 2$, while for the light detector $DP = 11$. As it will be shown in the next section, the pulse shape selection applied to the light detector allows one to tag α events with light yield compatible to that of β/γs, thus dramatically reducing the background.

2013 JINST 8 P05021

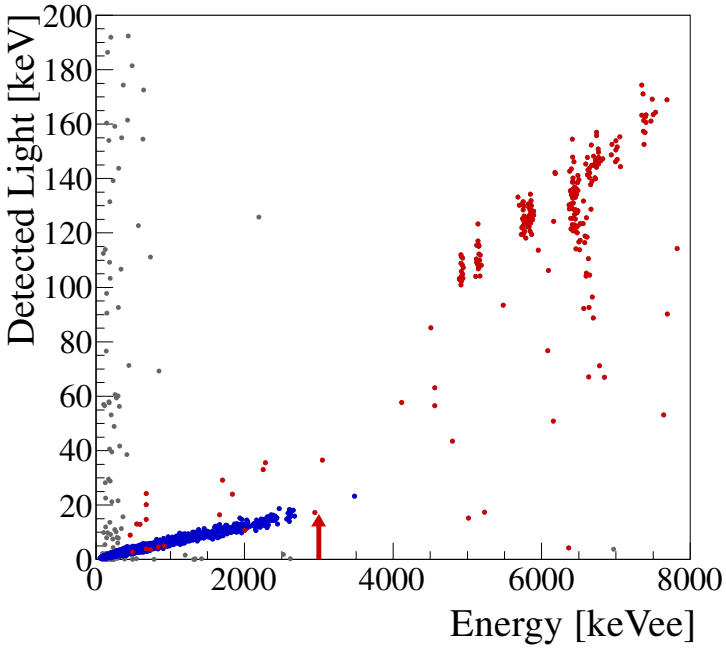

Figure 7. Data from 524 hours of background runs. The different colors mark β/γ events (blue) and α events (red) selected with pulse shape cuts on the light channel. The arrow points to the Q-value of the ^{82}Se decay. The gray dots indicate particles interacting in both the ZnSe and the light detector (double hit events), and events with no detected light (dark events). Double hit events are identified through their pulse shape in the LD, while dark ones through the shape in the ZnSe.

6 Background

We performed a background run of 524 hours in order to evaluate the internal contaminations of the crystal. To further decrease the environmental β/γ background, the crystal was shielded with ancient Roman lead, featuring an activity lower than 4 mBq/kg in ^{210}Pb [40]. Figure 7 shows the detected light as a function of the particle energy measured by the ZnSe. We notice that the pulse shape cuts allow to completely identify the interacting particle.

In figure 8 (right) the distribution of β/γ events is reported. We can identify the decay of ^{75}Se ($T_{1/2} = 119.779$ days, $Q = 863.6$ keV). ^{75}Se is produced via ^{74}Se neutron capture and decays via electron-capture (100%) with a complex combination of de-excitation γs and X-rays, producing a peak at ~ 410 keV and a series of peaks between 150 and 300 keV (figure 9).

We analyzed the decay rate of the 410 keV peak as a function of time, obtaining $T_{1/2}(^{75}\text{Se}) = 102 \pm 18$ days, which confirms our expectations. Another isotope that is produced by neutron activation in ZnSe is ^{65}Zn ($T_{1/2} = 244$ days, $Q = 1359.9$ keV). This isotope decays via electron capture and produces a peak at about 1350 keV. These contaminants do not contribute to the 0νDBD background of ^{82}Se, because of the low Q-value and the short half-life. The other events in the β/γ spectrum can be attributed to ^{40}K and ^{232}Th contaminations of the environment.

Finally, in the inset of figure 8 (right), the zoom on the energy region of interest of ^{82}Se is reported. One can see that only one event above 2615 keV is observed. This event, however, is in

2013 JINST 8 P05021

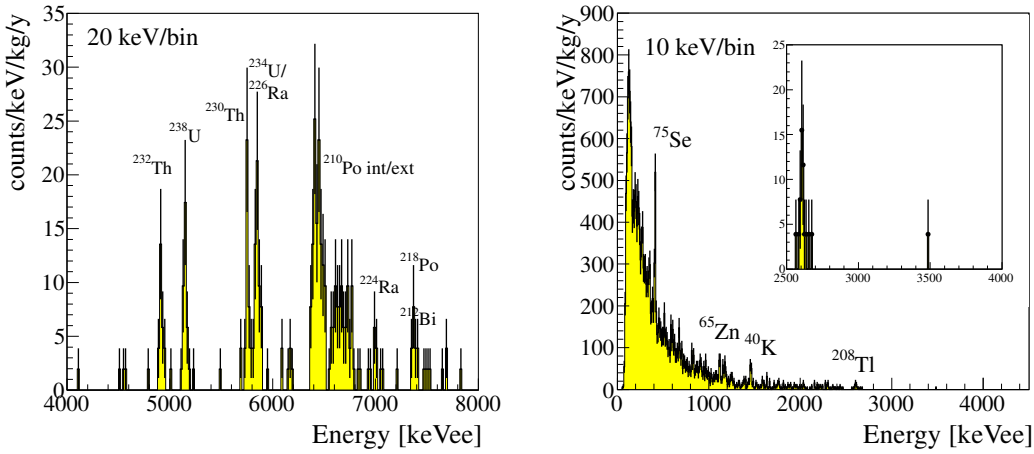

Figure 8. 524 h background run. Spectrum of α (left) and β/γ events (right). Data are calibrated using γ sources. αs result miscalibrated by +22% with respect to their nominal energy.

Table 3. Activity of the isotopes belonging to ^{232}Th and ^{238}U chains.

Chain	Nuclide	Activity [μBq/kg]
^{232}Th	^{232}Th	17.2 ± 4.6
	^{228}Th	11.1 ± 3.7
^{238}U	^{238}U	24.6 ± 5.5
	^{234}U	17.8 ± 3.3
	^{230}Th	24.6 ± 5.5
	^{226}Ra	17.8 ± 3.3
	^{210}Po	$< 90.9 \pm 10.6$

coincidence with high energy γ's seen by other scintillating crystals that we were testing in the same set-up. We believe that it can be ascribed to a muon interaction in the surrounding materials. This kind of events can be easily suppressed in bolometric arrays by applying time-coincidence cuts, as done in CUORICINO [2] or, ultimately, by surrounding the cryogenic facility with a muon veto.

In figure 8 (left) the α background is reported after cutting on both pulse shape and energy of the light channel. The activities of the most intense peaks, reported in table 3, show that ^{232}Th and ^{238}U are in equilibrium with their daughters.

In principle, a large internal contamination in ^{238}U could be worrisome because of one of its daughters, ^{214}Bi, which β-decays with a Q-value of 3272 keV. However, ^{214}Bi decays with a BR of 99.98% in ^{214}Po, which α-decays with a Q-value of 7.8 MeV. The half-life of ^{214}Po, which is about 160 μs, is extremely short compared to the time development of bolometric signals, which is hundreds of ms. For this reason, the β/γ emission of ^{214}Bi is simultaneously followed by a 7.8 MeV α particle and does not represent a problem for the background, as the superimposition of the two signals lies at much higher energies than the region of interest.

2013 JINST 8 P05021

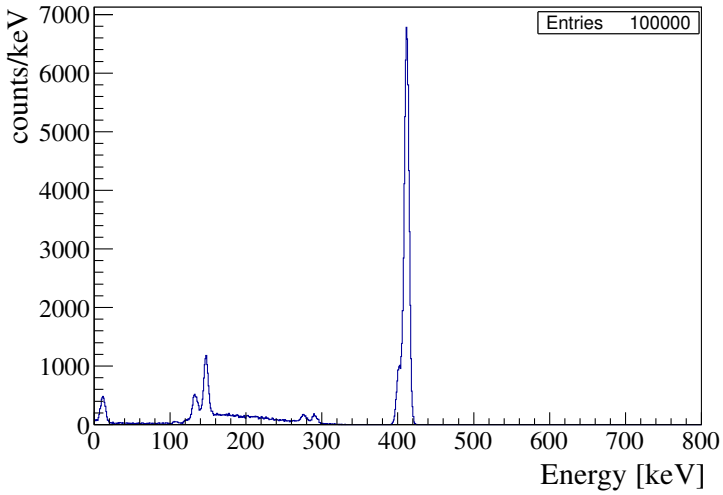

Figure 9. Simulation of the ^{75}Se decay in the ZnSe. Energy resolution set to 7 keV FWHM.

When evaluating the background due to ^{214}Bi we considered also its decay in ^{210}Tl, which occurs via α emission with a BR of 0.02 %. This contribution, however, can be easily suppressed: ^{210}Tl β-decays with a Q-value of 5489 keV and a half-life of 1.30 min. The background induced by the β emission can be rejected using the delayed coincidences with the α of ^{214}Bi. In this case, the dead time induced by the delayed coincidences is almost negligible, as the half-life of ^{210}Tl is very short and the BR for this decay is extremely small. As a consequence, even an internal contamination in ^{238}U of 25 μBq/kg would produce a background in the energy region of interest of only 3×10^{-4} counts/keV/kg/y.

A more dangerous background source is the one due to the internal contamination of ^{208}Tl, that belongs to the ^{232}Th chain and β-decays with a Q-value of 5001 keV.

Considering a ^{232}Th contamination of 17 μBq, we expect a background in the energy region of interest due to ^{208}Tl of about 2.5×10^{-3} counts/keV/kg/y, which represents the ultimate limit for the background. The background due to ^{208}Tl could be suppressed using the coincidences with its parent, ^{212}Bi, that α-decays with a half-life of 3 minutes. In this case, however, the introduced dead-time must be considered. A background reduction factor of 3, for example, requires a delayed coincidence of 10 min, which would imply a dead time of about 10%.

Summarizing, the internal contaminations of ^{214}Bi and ^{208}Tl do not represent a dangerous problem for the achievement of a background of 10^{-3} counts/keV/kg/y, which is the goal of the LUCIFER experiment. In any case, purification techniques are under study in order to reduce bulk contaminations of the crystals and, therefore, the dead time induced by delayed coincidences.

7 Conclusions

In this paper we analyzed the performances of a 431 g ZnSe crystal operated as scintillating bolometer. We measured the energy resolution at 2615 keV, close to the 0νDBD of ^{82}Se (2997 keV). By combining the light and heat signals, the resolution has been estimated as 13 keV FWHM.

2013 JINST 8 P05021

We presented the results of a 524 hours background run to identify the internal radioactive contaminations of the crystal. We measured ^{232}Th and ^{238}U contaminations of the order of tens of μBq/kg, which is compatible with the low background requirements of a 0νDBD experiment. In this run, no event passed the data analysis cuts against the background in the energy region of the decay, showing the potential of this detection technique.

We analyzed the scintillation properties of the detector and we demonstrated that the information carried by the light signal allows to identify the nature of the interacting particles in two different ways. Exploiting the different light yield of αs and β/γs, one can reject the background due to α particles within the energy region of interest for the ^{82}Se decay. We developed an algorithm, based on the shape of the light signals, to tag α particles with light yield compatible with β/γ ones.

Finally, the good identification of nuclear recoils at 100 keV allowed us to set the requirements for Dark Matter searches with ZnSe bolometric detectors. We estimated that nuclear recoils of ^{210}Po are detected with an amount of energy 35% greater than the nominal value, using a calibration function estimated from γ lines. This value has to be confirmed with dedicated tests, together with the evaluation of the calibration function of Zn and Se recoils. By using light detectors with baseline noise lower than 20 eV RMS, we estimate that β/γ events could be discriminated from nuclear recoils events of 10 keV, thus setting indicative requirements for Dark Matter searches in LUCIFER.

Acknowledgments

This work was partially supported by the LUCIFER experiment, funded by ERC under the European Union's Seventh Framework Programme (FP7/2007-2013)/ERC grant agreement n. 247115, funded within the ASPERA 2nd Common Call for R&D Activities. Thanks are due to the LNGS mechanical workshop and in particular to E. Tatananni, A. Rotilio, A. Corsi, and B. Romualdi for continuous and constructive help in the overall set-up construction. Finally, we are especially grateful to M. Guetti for his help.

References

[1] A. Alessandrello et al., *The first step toward CUORE: Cuoricino, a thermal detector array to search for rare events*, *Nucl. Phys. Proc. Suppl.* **87** (2000) 78.

[2] E. Andreotti et al., *^{130}Te Neutrinoless Double-Beta Decay with CUORICINO*, *Astropart. Phys.* **34** (2011) 822 [arXiv:1012.3266] [INSPIRE].

[3] R. Ardito et al., *CUORE: a cryogenic underground observatory for rare events*, hep-ex/0501010 [INSPIRE].

[4] CUORE collaboration, C. Arnaboldi et al., *CUORE: a cryogenic underground observatory for rare events*, *Nucl. Instrum. Meth.* **A 518** (2004) 775 [hep-ex/0212053] [INSPIRE].

[5] S. Rahaman et al., *Double-beta decay Q values of Cd-116 and Te-130*, *Phys. Lett.* **B 703** (2011) 412 [INSPIRE].

[6] M. Clemenza, C. Maiano, L. Pattavina and E. Previtali, *Radon-induced surface contaminations in low background experiments*, *Eur. Phys. J.* **C 71** (2011) 1805 [INSPIRE].

[7] S. Pirro et al., *Scintillating double beta decay bolometers*, *Phys. Atom. Nucl.* **69** (2006) 2109 [nucl-ex/0510074] [INSPIRE].

2013 JINST 8 P05021

[8] C. Arnaboldi et al., *$CdWO_4$ scintillating bolometer for Double Beta Decay: Light and Heat anticorrelation, light yield and quenching factors*, *Astropart. Phys.* **34** (2010) 143 [arXiv:1005.1239] [INSPIRE].

[9] C. Arnaboldi et al., *Characterization of ZnSe scintillating bolometers for Double Beta Decay*, *Astropart. Phys.* **34** (2011) 344 [arXiv:1006.2721] [INSPIRE].

[10] D.L. Lincoln et al., *First Direct Double-Beta Decay Q-value Measurement of 82Se in Support of Understanding the Nature of the Neutrino*, *Phys. Rev. Lett.* **110** (2013) 012501 [arXiv:1211.5659] [INSPIRE].

[11] L. Gironi et al., *Performance of $ZnMoO_4$ crystal as cryogenic scintillating bolometer to search for double beta decay of molybdenum*, 2010 *JINST* **5** P11007 [arXiv:1010.0103] [INSPIRE].

[12] J. Beeman et al., *Potential of a next generation neutrinoless double beta decay experiment based on ZnMoO4 scintillating bolometers*, *Phys. Lett.* **B 710** (2012) 318 [arXiv:1112.3672] [INSPIRE].

[13] J. Beeman et al., *Performances of a large mass ZnMoO(4) scintillating bolometer for a next generation 0vDBD experiment*, *Eur. Phys. J.* **C 72** (2012) 2142 [INSPIRE].

[14] J. Beeman et al., *ZnMoO4: a promising bolometer for neutrinoless double beta decay searches*, *Astropart. Phys.* **35** (2012) 813 [arXiv:1202.0238] [INSPIRE].

[15] S. Rahaman et al., *Q value of the Mo-100 Double-Beta Decay*, *Phys. Lett.* **B 662** (2008) 111 [arXiv:0712.3337] [INSPIRE].

[16] V. Ryzhikov, B. Grinyov, S. Galkin, N. Starzhinskiy and I. Rybalka, *Growing technology and luminescent characteristics of znse doped crystals*, *J. Cryst. Growth* **364** (2013) 111.

[17] P. Rudolph, N. Schäfer and T. Fukuda, *Crystal growth of znse from the melt*, *Mat. Sci. Eng.* **R 15** (1995) 85.

[18] S. Pirro, C. Arnaboldi, J. Beeman and G. Pessina, *Development of bolometric light detectors for double beta decay searches*, *Nucl. Instrum. Meth.* **A 559** (2006) 361 [INSPIRE].

[19] J. Beeman et al., *Effect of SiO2 coating in bolometric Ge light detectors for rare event searches*, *Nucl. Instrum. Meth.* **A 709** (2013) 22 [arXiv:1211.5548] [INSPIRE].

[20] K.M. Itoh et al., *Hopping conduction and metal-insulator transition in isotopically enriched neutron-transmutation-doped ^{70}Ge:Ga*, *Phys. Rev. Lett.* **77** (1996) 4058.

[21] S. Pirro, *Further developments in mechanical decoupling of large thermal detectors*, *Nucl. Instrum. Meth.* **A 559** (2006) 672 [INSPIRE].

[22] C. Arnaboldi, G. Pessina and S. Pirro, *The cold preamplifier set-up of CUORICINO: towards 1000 channels*, *Nucl. Instrum. Meth.* **A 559** (2006) 826 [INSPIRE].

[23] C. Arnaboldi et al., *The front-end readout for CUORICINO, an array of macro-bolometers and MIBETA, an array of mu-bolometers*, *Nucl. Instrum. Meth.* **A 520** (2004) 578 [INSPIRE].

[24] E. Gatti and P.F. Manfredi, *Processing the signals from solid state detectors in elementary particle physics*, *Riv. Nuovo Cimento* **9** (1986) 1.

[25] V. Radeka and N. Karlovac, *Least-square-error amplitude measurement of pulse signals in presence of noise*, *Nucl. Instrum. Meth.* **52** (1967) 86.

[26] G. Piperno, S. Pirro and M. Vignati, *Optimizing the energy threshold of light detectors coupled to luminescent bolometers*, 2011 *JINST* **6** P10005 [arXiv:1107.5679] [INSPIRE].

2013 JINST 8 P05021

[27] L. Cardani, S. Di Domizio and L. Gironi, *A BGO scintillating bolometer for gamma and alpha spectroscopy*, 2012 *JINST* **7** P10022 [arXiv:1208.5331] [INSPIRE].

[28] V. Tretyak, *Semi-empirical calculation of quenching factors for ions in scintillators*, *Astropart. Phys.* **33** (2010) 40 [arXiv:0911.3041] [INSPIRE].

[29] F.A. Danevich et al., *On the alpha activity of natural tungsten isotopes*, *Phys. Rev.* **C 67** (2003) 014310 [nucl-ex/0211013] [INSPIRE].

[30] G. Steigman and M.S. Turner, *Cosmological Constraints on the Properties of Weakly Interacting Massive Particles*, *Nucl. Phys.* **B 253** (1985) 375 [INSPIRE].

[31] M.W. Goodman and E. Witten, *Detectability of Certain Dark Matter Candidates*, *Phys. Rev.* **D 31** (1985) 3059 [INSPIRE].

[32] S. Di Domizio, F. Orio and M. Vignati, *Lowering the energy threshold of large-mass bolometric detectors*, 2011 *JINST* **6** P02007 [arXiv:1012.1263] [INSPIRE].

[33] L. Gironi, *Scintillating bolometers for Double Beta Decay search*, *Nucl. Instrum. Meth.* **A 617** (2010) 478 [arXiv:0911.1061] [INSPIRE].

[34] C. Arnaboldi et al., *A novel technique of particle identification with bolometric detectors*, arXiv:1011.5415 [INSPIRE].

[35] M. Carrettoni and M. Vignati, *Signal and noise simulation of CUORE bolometric detectors*, 2011 *JINST* **6** P08007 [arXiv:1106.3902] [INSPIRE].

[36] M. Vignati, *Model of the Response Function of Large Mass Bolometric Detectors*, *J. Appl. Phys.* **108** (2010) 084903 [arXiv:1006.4043] [INSPIRE].

[37] L. Gironi, *Pulse shape analysis with scintillating bolometers*, *J. Low Temp. Phys.* **167** (2012) 504.

[38] D. Moore et al., *Position and energy-resolved particle detection using phonon-mediated microwave kinetic inductance detectors*, *Appl. Phys. Lett.* **100** (2012) 232601 [arXiv:1203.4549] [INSPIRE].

[39] J.P. Filippini, *A Search for WIMP Dark Matter Using the First Five-Tower Run of the Cryogenic Dark Matter Search*, Ph.D. Thesis, University of California, Berkeley U.S.A. (2008).

[40] A. Alessandrello et al., *Measurements of internal radioactive contamination in samples of roman lead to be used in experiments on rare events*, *Nucl. Instrum. Meth.* **B 142** (1998) 163.

2013 JINST 8 P05021